Open access • Journal Article • DOI:10.1029/2002GB001891

Worldwide distribution of continental rock lithology: Implications for the atmospheric/soil CO2 uptake by continental weathering and alkalinity river transport to the oceans — Source link

Philippe Amiotte Suchet, Jean-Luc Probst, Wolfgang Ludwig

Institutions: University of Burgundy, Paul Sabatier University, University of Perpignan

Published on: 01 Jun 2003 - Global Biogeochemical Cycles (John Wiley & Sons, Ltd)

Topics: Soil production function, Weathering, Clastic rock, Sedimentary rock and Volcanic rock

Worldwide distribution of continental rock lithology: Implications for the atmospheric/soil CO_2 uptake by continental weathering and alkalinity river transport to the oceans

Philippe Amiotte Suchet
Microbiologie et Géochimie des Sols, UMR-INRA/Université de Bourgogne, Centre des Sciences de la Terre, Dijon, France

Jean-Luc Probst
Laboratoire des Mécanismes de Tranfert en Géologie, UMR-CNRS/Université Paul Sabatier, Toulouse, France

Wolfgang Ludwig
Centre de Formation et de Recherche sur l'Environnement Marin, Université de Perpignan, Perpignan, France

[1] The silicate rock weathering followed by the formation of carbonate rocks in the ocean, transfers CO_2 from the atmosphere to the lithosphere. This CO_2 uptake plays a major role in the regulation of atmospheric CO_2 concentrations at the geologic timescale and is mainly controlled by the chemical properties of rocks. This leads us to develop the first world lithological map with a grid resolution of $1^\circ \times 1^\circ$. This paper analyzes the spatial distribution of the six main rock types by latitude, continents, and ocean drainage basins and for 49 large river basins. Coupling our digital map with the GEM-CO2 model, we have also calculated the amount of atmospheric/soil CO_2 consumed by rock weathering and alkalinity river transport to the ocean. Among all silicate rocks, shales and basalts appear to have a significant influence on the amount of CO_2 uptake by chemical weathering.

KEYWORDS: lithological map, global carbon cycle, spatial distribution, river basins, riverine inputs to oceans, modeling

1. Introduction

[2] The significance of rock weathering in the global carbon cycle has already been discussed by many authors, such as *Berner et al.* [1983], *Meybeck* [1987], *Amiotte Suchet and Probst* [1993a, 1993b, 1995], *Ludwig et al.* [1998, 1999], *Gaillardet et al.* [1999]. Recently, it has been demonstrated that the riverine inputs of carbon to the ocean have to be taken into account in the regional distribution of sources and sinks of CO_2 in the ocean [*Aumont et al.*, 2001]. The chemical and physical erosion of land materials releases into rivers carbon which is subsequently discharged into the oceans (dissolved organic (DOC) and inorganic (DIC) carbon and particulate organic (POC) and inorganic (PIC) carbon). The present-day riverine flux of carbon is estimated to be about 1 Gt C yr^{-1} (0.8 to 1.2 according to literature estimates); DIC, PIC, DOC and POC fluxes represent, respectively, 38%, 17%, 25% and 20% of the overall carbon flux. Most of the carbon transported by the rivers originates from atmospheric CO_2, except PIC and half of the DIC which are supplied by the physical and chemical erosion of carbonates.

[3] The chemical erosion of inorganic materials consists in dissolving or hydrolyzing primary minerals of rocks and soils. The chemical reactions require CO_2 and release DIC, as can be seen, for example, in the equation for albite hydrolysis,

$$2NaAlSi_3O_8 + 2CO_2 + 11H_2O \rightarrow Al_2Si_2O_5(OH)_4 + 2HCO_3^- + 2Na^+ + 4H_4SiO_4, \quad (1)$$

or in the equation for the calcite dissolution,

$$CaCO_3 + CO_2 + H_2O \rightarrow Ca^{2+} + 2HCO_3^-. \quad (2)$$

[4] In river water, bicarbonates can be assumed to be equal to the alkalinity. All bicarbonate flux released by silicate hydrolysis (equation (1)) originates from the atmospheric CO_2, while it is only half for carbonate dissolution

Table 1. Proportions of Different Rock Types Exposed on the Continents as Calculated in This Work and Compared to Results From Other Studies

Rock Type	This Work	*Blatt and Jones* [1975]	*Meybeck* [1987]	*Gibbs and Kump* [1994]
Sandstones, sands	26.2	–	15.8	23.9
Shales	25.4	–	34.4	12.6
Carbonate rocks	13.4	–	15.9	9.3
Total sedimentary rocks	65.0	66.0	66.1	45.8
Intrusive igneous rocks	–	9.0	–	–
Metamorphic rocks	–	17.0	–	–
Total shield rocks (intrusive igneous + metamorphic)	27.5	26.0	26.0	20.0
Acid volcanic rocks	2.3	–	3.8	–
Basalts	5.2	–	4.1	–
Total volcanic rocks	7.5	8.0	7.9	6.8
Total crystalline rocks	35.0	34.0	33.9	26.8
Fold belts	–	–	–	27.5
Total	100.0	100.0	100.0	100.1

(equation (2)). The flux of CO_2 that is consumed by weathering processes is mainly produced by soil organic matter oxidation,

$$CH_2O + O_2 \rightarrow CO_2 + H_2O. \quad (3)$$

[5] On a geological timescale, the fluxes of CO_2 consumed by carbonate dissolution (equation (2)) on the continents are balanced by the CO_2 fluxes released to the atmosphere by carbonate precipitation in the oceans. Consequently, with regard to the CO_2 content in the atmosphere, it is only the fluxes of CO_2 consumed by silicate rock weathering which represent a net sink of CO_2. This is the reason why future research on weathering must take into account the relative outcrop abundance of silicate and carbonate rocks when investigating the CO_2 uptake by silicate rock weathering and the subsequent riverine alkalinity transport. Recently, *Dessert et al.* [2001] have shown the impact of the Deccan Traps, one of the largest continental flood basalts (65.5 Myr ago), on chemical weathering and atmospheric CO_2 consumption on Earth. They estimated that the weathering of Deccan Traps basalts could be responsible for a 20% reduction of CO_2 content in the atmosphere, accompanied by a global cooling of 0.55°C. This result underlines the major role that the basalt outcrop abundance on Earth could play on the global carbon cycle and on the climatic evolution of the Earth.

[6] In this paper, we will examine the influence of the abundance of the different rock types on the atmospheric/soil CO_2 uptake by rock weathering and on the riverine transport of inorganic carbon to ocean. Until now, the spatial distribution of outcrop abundance for the different rock types has not been well known in detail at a global scale.

[7] The main difficulty in constructing a global data set of rock type exposures on the continents is that the information given by geological maps is inadequate. Indeed, geological maps focus on the age of rocks (for sedimentary rocks), on their deformation and on their structural position (sedimentary basin, mountain range, etc.), but information concerning the chemical and physical nature of rocks is often insufficient. This lack of information is problematic, especially for the chemical composition of sedimentary rocks, which is highly variable. Shield rocks are quite homogeneous from a chemical point of view.

[8] Few studies attempted to estimate the abundance of various rock types on the continents, and these estimates evolved with the knowledge in geology and the available data during the last century. In a first summary, *Clarke* [1924] proposed that continental outcrops were composed of 75% of sedimentary rocks and of 25% of combined igneous and metamorphic rocks. The first modern estimates have been proposed by *Blatt and Jones* [1975]. They established that the land surfaces were composed of 8% of extrusive crystalline rocks, 9% of intrusive crystalline rocks, 17% of metamorphic and precambrian crystalline rocks and 66% of sedimentary rocks. To do so, they used a sampling technique generating 3000 points, distributed over the entire land area. *Blatt and Jones* [1975] themselves noticed that the information collected for sedimentary rocks did not allowed to characterize them precisely. *Meybeck* [1987] greatly refined these results with calculations based on volume estimates determined by *Ronov and Yaroshevskyi* [1972, 1976] and taking into account of the wide diversity of sedimentary rocks (see Table 1).

Table 2. Lithological Description of the Six Rock Types Composing the Present-Day Lithological Map

Category	Description
Sand and sandstones	eolian, fluvial and marine sandy sediments not carbonated: mainly sands, sandstones and conglomerates
Shales	clastic and argilaceous sediments of various origin, not or poorly carbonated: clays, clay-shales, evaporites, . . .
Carbonate rocks	all rocks with more than 50% of carbonate minerals: mainly limestones, marls, dolomites and metamorphic limestones
Shield rocks	commonly every rocks composing shield regions: intrusive and metamorphic acid rocks (schists, micaschists, gneisses, granites, granodiorites, diorites)
Acid volcanic rocks	effusive acid rocks: mainly rhyolites and similar volcanic rocks
Basalts	effusive basic rocks more or less differentiated (mainly basalts s.l., dolerites and andesites) + igneous basic rocks (gabbros)

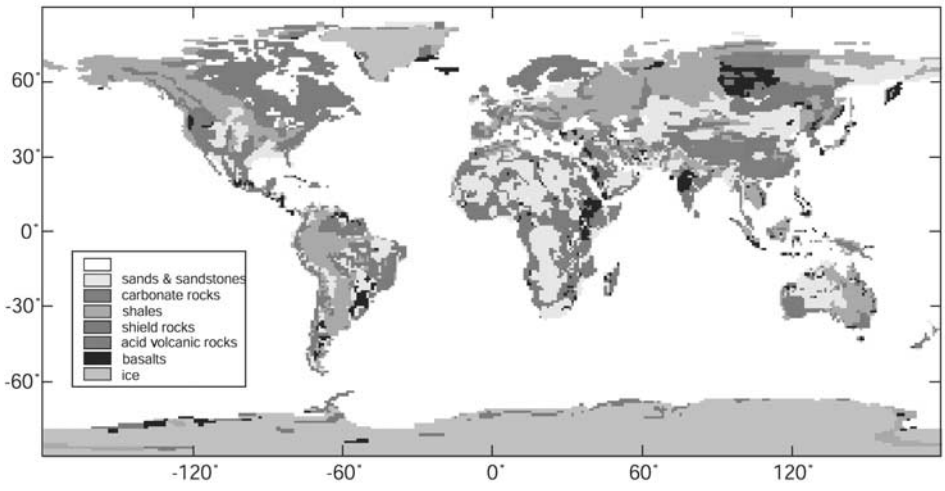

Figure 1. Present-day exposures of the six major rock types on land area (1° × 1° resolution). See color version of this figure at back of this issue.

[9] However, all these results do not take into account the spatial distribution of rock types, which is essential in the study of the weathering of these rocks at the global scale. *Bluth and Kump* [1991] made a very original work on the construction of paleogeologic maps and proposed a world map for what they called "the recent," with a resolution of 2° by 2°. This map corresponds to the Pliocene period and should be very close to a present-day map without Quaternary exposures. This map has been refined by *Gibbs and Kump* [1994] in order to correct for underrepresentation of shield rocks. Their calculations for global exposures are given in Table 1.

[10] The lithological associations that *Gibbs and Kump* [1994] distinguished are sandstones, shales, carbonate rocks, extrusive igneous rocks (i.e., volcanic rocks), shield rocks and fold belts. Two comments can be made concerning this map: The first one is that it has not been constructed from the observation of the present-day exposures, which could lead to some discrepancies. The second one is that about 27% of the total exposures are defined as "fold belts" and cannot be precisely characterized. Consequently, compared to the results of *Blatt and Jones* [1975] and *Meybeck* [1987], the work of *Gibbs and Kump* [1994] underestimates shield rock and sedimentary rock exposures (Table 1). This could be explained by the inclusion of sedimentary and shield rocks in the fold belts category.

[11] Consequently, the first objective of this paper is to propose a worldwide lithological map in a numeric format with a grid resolution of 1° × 1°. The basic data will be available on a web site and could be used in future researches on global biogeochemical cycles. The second objective is to estimate what is the impact of the abundance and distribution of the rock outcrops on the present-day rate of CO_2 consumed by rock weathering and on riverine alkalinity fluxes.

2. Data and Methods

[12] In this work, we have built a global map of the main rock types exposed on the continental areas today. This map has been constructed and digitized from synthetic lithological and soil maps published by the *Food and Agriculture Organization* (*FAO-UNESCO*) [1981] for each continent. These maps constitute the basis of our lithological map. Although the scale used by FAO-UNESCO to represent the maps is very coarse (about $1/50 \times 10^6$), we consider that it is sufficient to build up a global numeric map with a resolution of 1° by 1° (i.e., a square of about 111 by 111 km on the equator). The FAO-UNESCO synthetic lithological maps provide quite complete and precise information about the general lithology of continental areas for Central and South America, Africa, Asia and Australia, which allows us to distinguish carbonate rocks, shales and sands and sandstones among the sedimentary rocks. However, for North America and Europe, lithological information is often not accurate enough to identify separately carbonates, shales and sandstones. Finally, the FAO-UNESCO maps do not include Antarctica. Therefore, additional information has been collected from various sources. Notably, the UNESCO World Geological Atlas [*Choubert and Faure-Mauret*, 1981] has been used to complete the outlines of some geological formations and to build a comprehensive lithologic map for the ice free area of Antarctica. In addition, the paleogeographical maps of Ronov and coworkers [*Ronov and Khain*, 1961; *Khain et al.*, 1975; *Ronov et al.*, 1979], concerning the Mesozoic and Cenozoic periods, have been consulted to complete the lithology of the sedimentary units reported by FAO-UNESCO for Europe and North America.

[13] Obviously, the lithological description of sedimentary units varies from one source to another, which leads us to form large groups. We have distinguished very few different categories of rock types, which are sands and sandstones, shales, carbonate rocks, combined intrusive igneous rocks and metamorphic rocks (i.e., shield rocks), acid volcanic rocks, and basalts. A brief description of each category is given in Table 2.

[14] These rock categories have been first defined according to the available information and they also reflect the chemical composition and the behavior of rocks with regard

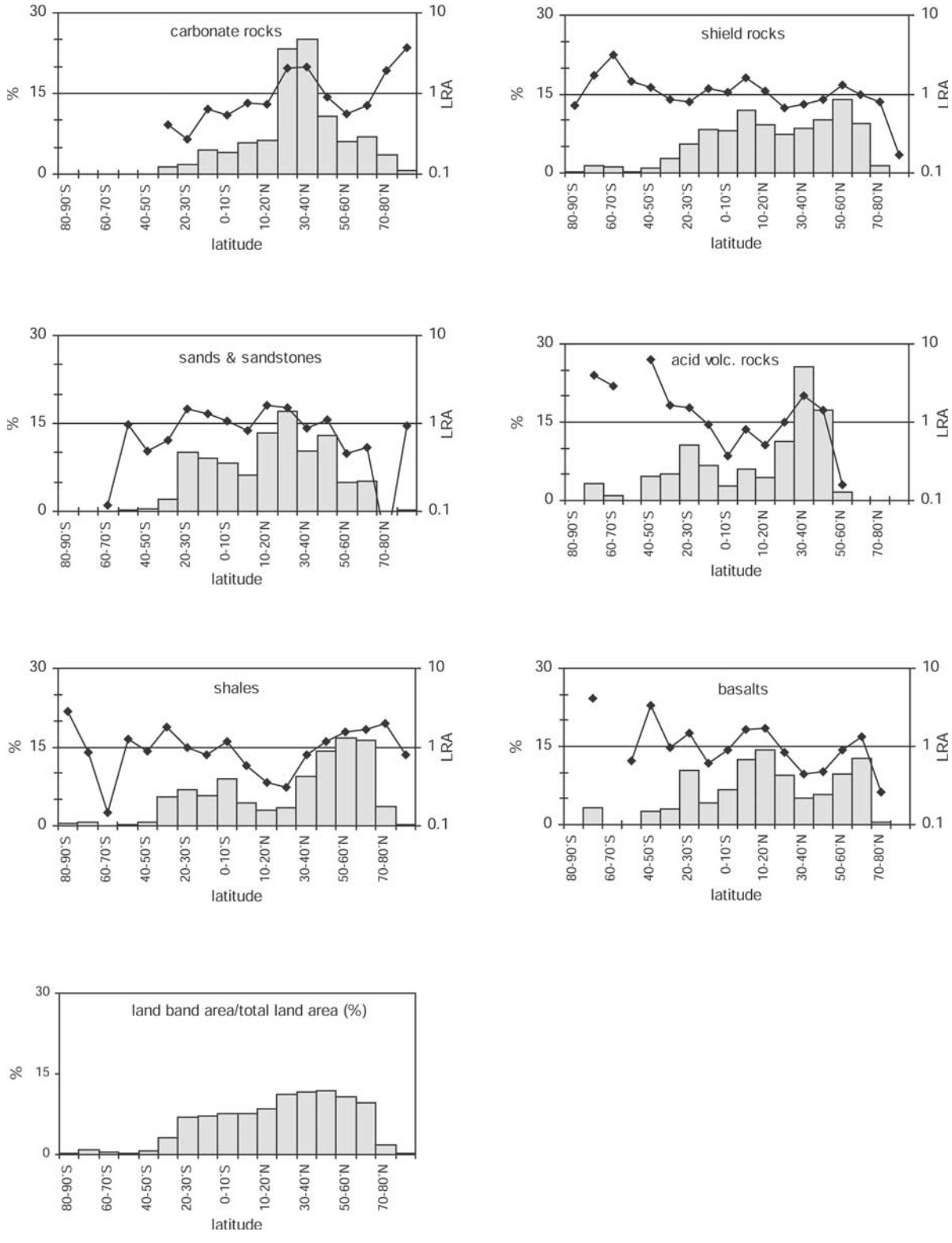

Figure 2. Latitudinal distribution of major rock types outcropping on land areas. Left Y axis and bar chart: ratio (in percent) of the rock type area at a given latitude to its worldwide area. Right Y axis and black curve: Latitudinal Relative Abundance: ratio (in percent) of the latitudinal proportion of rock type area (i.e., the percentage of the latitudinal land area occupied by a given rock type) to the latitudinal proportion of total land areas (i.e., the percentage of the world wide land area located at the given latitude). A LRA ratio below 1 means that the rock type is underrepresented; when it is above 1, the rock type is overrepresented.

Table 3. Relative Abundance of the Six Different Rock Types Exposed on Land by Continent (Endoreic and Exoreic Area) and by Ocean Drainage Basins[a]

	Sands and Sandstones		Shales		Carbonate Rocks		Shield Rocks		Acid Volcanic Rocks		Basalts		Total Land Areas	
	a	b	a	b	a	b	a	b	a	b	a	b	Percent of Land Area Without Ice	Percent of Land Area With Ice
Africa exoreic	19.8	38.5	0.3	0.6	12.2	12.1	20.9	42.6	0.0	0.0	16.4	6.2	13.5	12.2
Africa endoreic	23.0	55.9	1.2	2.8	14.5	17.9	7.7	19.7	0.0	0.0	7.7	3.7	10.8	9.8
Africa total	42.8	46.3	1.5	1.6	26.7	14.7	28.6	32.4	0.0	0.0	24.0	5.1	24.3	22.0
Antarctic	0.0	0.8	1.2	23.3	0.0	0.0	2.6	54.8	4.1	7.2	3.5	13.9	1.3	9.4
Asia exoreic	17.2	19.4	29.5	31.9	27.1	15.4	20.4	24.0	6.7	0.7	39.3	8.6	23.4	21.2
Asia endoreic	11.7	49.2	3.6	14.5	7.6	16.2	4.2	18.6	0.0	0.0	1.8	1.5	6.3	5.7
Asia total	28.9	25.7	33.0	28.2	34.6	15.6	24.6	22.9	6.7	0.5	41.1	7.1	29.7	26.9
Australia exoreic	1.7	14.3	6.2	50.1	0.3	1.1	2.8	24.2	4.4	3.1	4.4	7.2	3.2	2.9
Australia endoreic	5.5	51.0	2.7	24.1	1.4	6.7	1.5	14.5	4.3	3.4	0.2	0.3	2.8	2.6
Australia total	7.2	31.7	8.9	37.8	1.7	3.7	4.3	19.6	8.7	3.3	4.6	3.9	6.0	5.4
Europe exoreic	2.8	11.0	11.8	44.5	7.4	14.8	6.3	26.0	1.5	0.5	4.2	3.2	6.7	6.1
Europe endoreic	0.5	6.6	5.5	71.2	3.2	21.8	0.0	0.0	0.0	0.0	0.1	0.4	2.0	1.8
Europe total	3.3	10.0	17.3	50.5	10.7	16.4	6.3	20.1	1.5	0.4	4.3	2.6	8.7	7.9
North America exoreic	7.3	11.6	18.4	28.4	22.4	18.3	19.7	33.1	42.7	5.9	8.4	2.6	16.4	16.1
North America endoreic	0.1	7.9	0.0	0.0	0.0	0.0	0.0	0.0	10.7	92.1	0.0	0.0	0.3	0.2
North America total	7.3	11.6	18.4	28.0	22.4	18.0	19.7	32.6	53.4	7.3	8.4	2.6	16.7	16.3
South America exoreic	10.3	20.9	19.0	36.9	3.9	4.0	13.7	28.9	21.8	3.8	14.1	5.6	13.1	11.8
South America endoreic	0.0	2.7	0.5	46.3	0.0	0.0	0.2	22.2	3.7	28.7	0.0	0.0	0.3	0.3
South America total	10.4	20.5	19.6	37.1	3.9	3.9	13.9	28.8	25.5	4.3	14.1	5.4	13.3	12.1
Total exoreic	59.2	20.1	86.4	28.2	73.3	12.6	86.3	30.7	81.3	2.4	90.3	6.0	77.6	79.7
Total endoreic	40.8	47.9	13.6	15.3	26.7	15.9	13.7	16.8	18.7	1.9	9.7	2.2	22.4	20.3
Total	100.0	26.3	100.0	25.3	100.0	13.4	100.0	27.6	100.0	2.3	100.0	5.1	100.0	100.0
Arctic Ocean	11.2	14.3	25.5	45.9	14.4	11.6	10.9	21.4	0.0	0.0	17.9	6.9	15.7	14.0
North Atlantic	21.0	16.7	24.3	27.2	30.0	15.0	30.4	36.9	20.1	1.9	9.7	2.3	25.3	23.6
South Atlantic	28.2	34.5	8.6	14.9	8.8	6.8	19.8	37.1	7.4	1.1	15.3	5.6	16.4	14.4
Pacific	15.5	16.2	20.1	29.6	18.4	12.1	17.6	28.1	55.3	6.8	23.5	7.3	19.3	17.0
Indian Ocean	19.6	25.4	11.3	20.5	20.7	16.9	13.3	26.3	10.3	1.6	24.2	9.4	15.5	13.6
Mediterranean	4.5	14.5	8.9	39.7	7.6	15.3	5.0	24.5	1.9	0.7	5.5	5.3	6.3	5.5
Below 60° south	0.1	0.8	1.4	23.3	0.0	0.0	3.0	54.8	5.1	7.2	3.8	13.9	1.7	11.8
Total	100.0	20.1	100.0	28.2	100.0	12.6	100.0	30.7	100.0	2.4	100.0	6.0	100.0	100.0

[a]Column a is percent of the total area of each rock type, and column b is percent of the area of each continent or each ocean drainage basin.

to the chemical weathering. For example, as shown by *Amiotte Suchet and Probst* [1993a, 1993b], basic igneous rocks (basalts, gabbros) are, on average, more rapidly weathered than acid volcanic rocks, which are themselves less resistant than granites and gneisses. One of the most important points in the definition of rock categories is the presence of carbonate minerals. Several authors have demonstrated that weathering rates exponentially increased with the amount of carbonate minerals in rocks (among other, *Peters* [1984], *Meybeck* [1987], *Amiotte Suchet and Probst* [1993a, 1993b], and *Gibbs and Kump* [1994]). Therefore, rocks containing significant amounts of carbonate minerals are classified as carbonate rocks (Table 1). However, because of the coarse scale at which information has been collected (this information is necessarily simplified), carbonate minerals can sometimes be present in sedimentary rocks other than strictly carbonate rocks. As already emphasized by *Amiotte Suchet and Probst* [1993a, 1993b, 1995] and *Gibbs and Kump* [1994], the mineralogical composition of shales is highly variable, notably with respect to the presence and the proportion of carbonate minerals. In this work, it can be considered that shales include different argilaceous and clastic rocks, which can contain up to 50% of carbonate mineral. In practice, well-identified carbonate rocks (limestones, dolomites, marls, metamorphic limestones) have been classified as ''carbonate rocks'' and well-identified noncarbonated clastic sediments have been classified as ''sand and sandstones.'' The remaining ''suspect'' sedimentary rocks have been classified together with argilaceous sedimentary rocks as ''shales.''

[15] Compared to the 18 major rock types that have been distinguished by *Meybeck* [1987], our six categories may be considered as oversimplified. However, it will be demonstrated below that these are sufficient to be used in the quantification of global erosion. Nevertheless, some shortcomings can be noticed. Evaporitic rocks, which are not clearly described in the sources we used (probably because their occurrence is highly variable in space), have been included in shales. This is an obvious problem that must be addressed in the future because gypsum and rock salt deposits composing evaporites are easily dissolved and affect significantly river transport of dissolved solids. Finally, in the following, the results concerning acid volcanic rocks should be cautiously interpreted because outcrops are often very small and do not always appear at the scale we worked.

3. Spatial Distribution of Different Rock Types Over the Continents

3.1. Worldwide Abundance of Major Rock Types

[16] The $1° \times 1°$ lithological world map developed in this work is presented in Figure 1. The basic data are available at http://www.obs-mip.fr/omp/umr5563/4equ/hg/IGCP459/

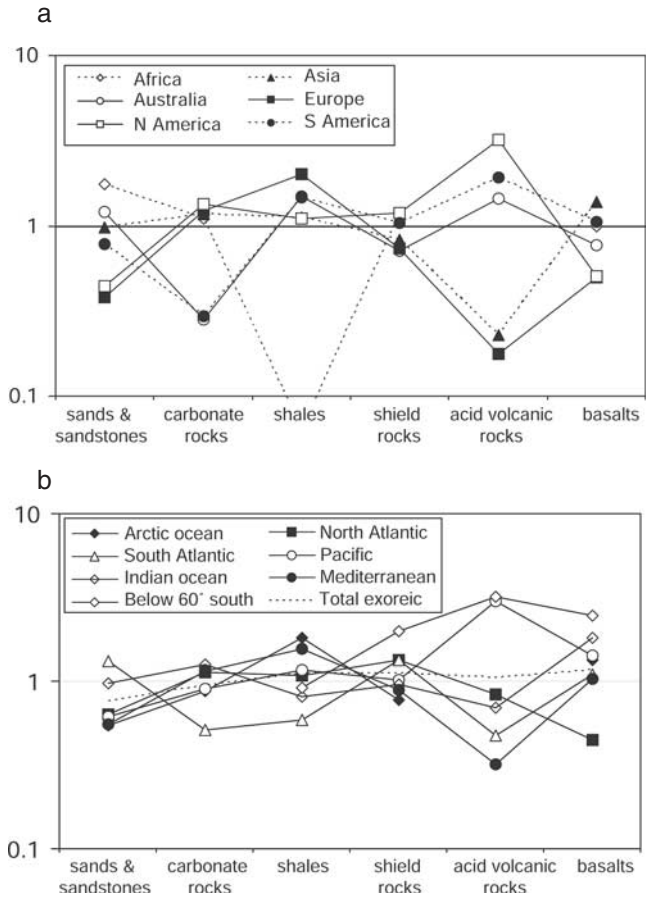

Figure 3. Relative abundance of rock types (a) on each continent and (b) on each ocean drainage basin normalized to the relative abundance of rock types on the total land areas (calculations have been executed considering total continental areas without ice).

litho.html. Using this digitized map, the outcrop areas of each rock type on land have been calculated and their relative abundance is presented in Table 1. Concerning the proportion of total sedimentary (one third) and crystalline rocks (two thirds), our results are very close to those of *Blatt and Jones* [1975] and of *Meybeck* [1987]. This confirms that the calculations made by *Gibbs and Kump* [1994] should be corrected by the redistribution of the fold belts toward shield rocks (about 7%) and toward sedimentary rocks (about 20%). Inside these two main categories, our estimates are in agreement with those of *Meybeck* [1987], except for clastic rocks. Indeed, the equivalent proportions of sands/sandstones and shales differ from those of *Meybeck* [1987], who proposed that shales are 2 times more abundant than sands and sandstones. This difference is probably due to the basis data used by *Meybeck* [1987] from *Ronov and Yaroshevskyi* [1972, 1976], who have considered sandstones sensus stricto and who probably grouped together sands and shales. This could indicate that the proportion of sands represents about 10%.

[17] The latitudinal distribution of each lithology (Figure 2), based on the map developed in this work, shows that all rock types are present at almost all latitudes but their relative abundance is highly variable from one latitude to an other. Figure 2 compares for each rock type the outcrop abundance by latitude with the distribution of land areas using a Latitudinal Relative Abundance (LRA) ratio (see Figure 2 caption for more explanation). A LRA ratio below 1 means that the rock type is underrepresented; when it is above 1, the rock type is overrepresented. It can be observed that shield rocks and sand/sandstones are equally distributed compared to the land areas (except for the high latitudes), whereas the other rocks exhibit higher or lower LRA according to the latitude. Most of the carbonate rocks (about 60%) are distributed between 20°N and 50°N. They appear to be overrepresented in comparison with the proportion of land areas, not only between 20°N and 40°N, but also at the higher northern latitudes (70°N–90°N). Shales are more abundant between 30°N and 70°N and between 0° and 40°S. The minimum LRA ratio observed between 0° and 30°N mainly corresponds to the African continent. Concerning the volcanic rocks (basalts and acid volcanic rocks), their latitudinal distribution is more heterogeneous than for the other rocks. More than half of the acid volcanic rocks outcrops between 20°N and 50°N, but their LRA is also rather important for the southern latitudes (20°S–50°S). The basalts are distributed over three main latitudinal zones: 36% between 0° and 30°N (Deccan Traps and Ethiopia), 23% between 50°N and 70°N (Iceland, Siberia and Kamchatka) and 10% between 20°S and 30°S (Parana Traps).

[18] The surface exposures of the different rock types can be also calculated for each continent, considering exoreic and endoreic areas, and for each oceanic basin (Table 3 and Figure 3). Most of sands and sandstones are located in Africa and in Asia, with a nonnegligible part that are not drained toward the ocean (endoreic areas). Shales follow more or less the proportion of the continental surfaces, except for Africa, where they are poorly represented, and for Europe, where they are largely represented (Figure 3a). Carbonate rocks show a homogeneous distribution, except for Australia and South America where outcrops are quite sparse. Shield rocks (plutonic and metamorphic rocks) follow quite closely the proportion of continental surfaces. The location of basalts is related to the occurrence of the trap structures (Deccan and Siberia in Asia, Parana in South America), and consequently they are poorly represented in Europe and North America. The acid volcanic rocks present a more heterogeneous distribution over the different continents: highly represented in North and South America and Australia, very poorly represented in the other continents.

[19] Finally, when looking at ocean drainage basins (Figure 3b), the distribution is more homogeneous than for the continents, except for volcanic rocks. Nevertheless, each ocean drainage basin presents a substantial enrichment or depletion for at least one rock type, which is very important to take into account with regard to the weathering products released to the rivers and transported into the ocean. Indeed, the waters flowing into the South Atlantic Ocean are draining continental areas depleted in shales, carbonates and acid volcanic rocks. The Pacific Ocean drainage basin is enriched in acid volcanic rocks

Table 4. Lithological Composition of 40 Major River Basins of the World (in Percent of the Basin Area)

	Basin Number	Area, 10^6 km^2	Runoff,[a] km^3 yr^{-1}	Sands and Sandstones	Shales	Carbonate Rocks	Shield Rocks	Acid Volcanic Rocks	Basalts
Amazon	1	5.83	6223	16.7	50.7	3.9	26.8	1.9	0.0
Amour	2	1.87	407	11.9	28.0	0.0	53.6	0.0	6.5
Colorado	3	0.67	28	55.6	0.0	0.0	10.4	34.0	0.0
Columbia	4	0.62	269	1.4	12.9	0.0	43.9	33.4	8.4
Danube	5	0.74	140	3.3	66.7	14.5	15.5	0.0	0.0
Don	6	0.39	31	0.0	94.1	5.9	0.0	0.0	0.0
Fraser	7	0.24	104	0.0	68.8	0.0	21.7	9.5	0.0
Ganges-Brahmaputra	8	1.64	1313	15.4	31.5	33.8	18.0	0.0	1.4
Godavari	9	0.30	147	3.9	0.0	0.0	61.6	0.0	34.5
Huangho	10	0.79	41	27.6	5.9	7.6	58.9	0.0	0.0
Yenisei	11	2.44	665	6.4	12.3	6.9	38.4	0.0	36.0
Indigirka	12	0.34	54	39.9	60.1	0.0	0.0	0.0	0.0
Indus	13	0.88	251	16.8	24.0	26.0	33.1	0.0	0.0
Irrawaddi	14	0.40	459	30.6	14.1	44.0	11.3	0.0	0.0
Kolyma	15	0.59	122	72.3	27.7	0.0	0.0	0.0	0.0
Lena	16	2.32	393	10.8	38.7	11.2	34.2	0.0	5.1
Limpopo	17	0.31	27	25.0	0.0	14.2	39.2	0.0	21.6
Mackenzie	18	1.47	260	0.0	53.9	20.6	25.5	0.0	0.0
Magdalena	19	0.26	313	23.8	28.5	4.8	23.8	19.1	0.0
Mekong	20	0.82	623	8.4	43.2	21.4	18.2	2.9	5.8
Mississippi	21	3.13	570	25.3	47.6	18.1	8.7	0.3	0.0
Murray	22	1.11	40	0.9	72.3	0.0	21.2	2.7	2.9
Niger	23	1.50	166	57.8	0.0	6.3	35.1	0.0	0.8
Nile	24	1.84	125	31.9	0.0	2.5	45.1	0.0	20.4
Ob	25	3.01	477	19.8	71.9	2.7	2.7	0.0	3.0
Orange	26	0.66	26	68.8	0.0	9.8	16.5	0.0	4.8
Orinoco	27	0.96	759	17.7	46.8	1.3	30.4	0.0	3.8
Parana	28	2.84	666	27.3	43.9	1.2	14.5	0.8	12.3
Sao Francisco	29	0.59	119	14.0	8.0	39.8	38.1	0.0	0.0
Senegal	30	0.36	15	64.5	3.2	0.0	29.1	0.0	3.3
Severnaia Dvina	31	0.30	97	10.9	78.4	10.8	0.0	0.0	0.0
Si Kiang	32	0.44	419	0.0	0.0	82.4	17.6	0.0	0.0
St. Lawrence	33	0.87	360	0.0	6.1	24.9	69.0	0.0	0.0
Tigris-Euphrates	34	0.93	156	17.2	25.8	42.5	2.2	11.3	1.0
Yana	35	0.21	25	50.6	49.4	0.0	0.0	0.0	0.0
Yangtze-Kiang	36	1.74	908	13.9	7.9	44.0	34.2	0.0	0.0
Yukon	37	0.78	169	0.0	85.4	0.0	14.6	0.0	0.0
Zaire	38	3.60	1298	46.6	0.0	10.1	41.9	0.0	1.4
Zambesi	39	1.31	109	45.9	0.0	13.6	38.7	0.0	1.8
Total 39 selected basin		49.11	18 379	22.3	32.2	11.8	27.1	1.6	5.0

[a]According to our digitized runoff map (discussed by *Ludwig et al.* [1998, 1999]) from the Atlas of World Water Balance [*Korzoun et al.*, 1977].

and depleted in sands and sandstones. The Mediterranean is depleted in acid volcanic rocks and in sands and sandstones. The North Atlantic drainage basin is depleted in sands/sandstones and in basalts. Finally, the Indian Ocean drainage basin is only enriched in basalts due to the Deccan Traps and to the Ethiopia, and the continental areas draining below 60°S are enriched in shields and volcanic rocks.

3.2. Average Lithology of Large River Basins

[20] The lithological composition of 39 large river basins has been determined on the basis of drainage basin limits defined by *Pinet and Souriau* [1988] and *Ludwig et al.* [1996]. We limited the calculations to river basins comprising at least 20 grid cells of 1° by 1° in order to avoid errors caused by the resolution of the lithological map compared to the river basin size. Results (Table 4) show that the average lithological composition calculated for the set of selected river basins is close to that of the whole continental area (Table 1) showing that the set of drainage basins is representative of the worldwide distribution of the different rocks types. Nevertheless, inside the sedimentary rocks, sands and sandstones as well as carbonate rocks are somewhat underrepresented on the set of river basins with regard to the world average.

[21] As seen in Table 4 and Figure 4, the percentage of each rock type is greatly variable from one river basin to another. If one groups together the different rock types according to their chemical alterability and their CO_2 consumption rate (high rate for carbonates, moderate rate for basalts plus shales and low rate for shields plus sands/sandstones), three sets of river basins can be distinguished (Figure 4). The first group represents the highest percentage of carbonates (20 to 80%) and comprises most of the Himalayan rivers (Si-Kiang, Yangtze, Irrawady, Indus, Mekong) plus the St. Lawrence, the Tigris-Euphrate and the Sao Francisco. The other two groups have less than 20% of carbonates, one dominated by shields and sands/sandstones (at least 60%) which comprises most of the African rivers, and the other one by shales and basalts (at least 40%)

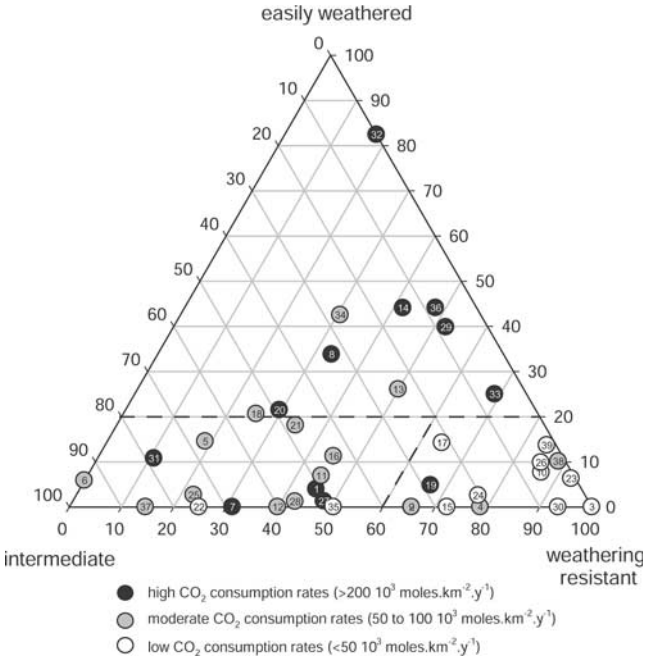

Figure 4. Typology of the major river drainage basins according to their lithological characteristics and to their weathering CO_2 consumption rates (numbers in circles refers to basin numbers in Table 4). Easily weathered rocks: carbonate rocks; intermediate: basalts, shales; weathering resistant: shield rocks, acid volcanic rocks, sands and sandstones.

which includes most of the Siberian and North and South American rivers.

4. Implication for Global Atmospheric/Soil CO_2 Consumed by Weathering

4.1. Lithology and Atmospheric/Soil CO_2 Consumed by Weathering: The GEM CO_2 Model

[22] The flux of atmospheric/soil CO_2 consumed by rock weathering (F_{CO2}) is mainly a function of runoff (Q) and of the rock type that is drained by surface water, as already demonstrated by *Amiotte Suchet and Probst* [1993a, 1993b, 1995]. Empirical relationships were established using data published by *Meybeck* [1986] concerning runoff and alkalinity concentrations of 232 monolithologic watersheds in France. These watersheds were grouped into the main six categories of rocks outcropping on the continents as described in Table 2. For each watershed, F_{CO2} fluxes were determined considering that for streams draining silicate rocks, F_{CO2} was equal to the whole alkalinity flux, and for streams draining carbonate rocks, F_{CO2} was equal to half of the alkalinity flux. Then, linear models between F_{CO2} and Q were determined for each of the six rock categories (Figure 5). These relationships form the Global Erosion Model for atmospheric/soil CO_2 consumed by chemical weathering (GEM-CO2 [*Amiotte Suchet and Probst*, 1995]). As seen in Figure 5, F_{CO2} increases as runoff increases but with a different rate according to the rock type. Similar relationships have been proposed by *Gibbs and Kump* [1994] using the data on North American streams. Thus, F_{CO2} is 17 times higher on carbonate rocks than on shield rocks. F_{CO2} consumed by weathering of the other rock types ranges between these two extremes. It must be noticed that F_{CO2} is twice as high for the weathering of basalts as for the weathering of acid volcanic rocks, although these rocks are structurally very similar.

[23] The GEM-CO2 model calculates F_{CO2} at a continental scale using our lithological map and the global distribution of runoff digitized from the UNESCO Atlas of World Water Balance [*Korzoun et al.*, 1977] and is discussed in detail by *Ludwig et al.* [1998, 1999]. In the GEM-CO2 model, it is assumed that sands and sandstones, shield rocks, basalts, acid volcanic rocks and shales are strictly silicate rocks and do not contain any carbonate minerals. That means that all bicarbonates ions are considered to come from the atmospheric/soil CO_2. This assumption is not correct, of course, especially for shales which can contain a nonnegligible but highly variable proportion of

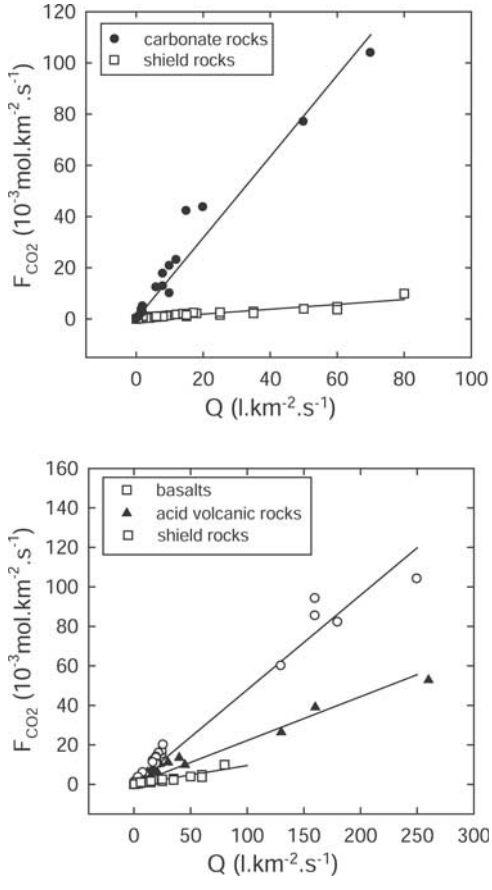

Figure 5. Linear models between the flux of CO_2 consumed by weathering (FCO_2) and the drainage intensity (Q) determined for the main rock categories (after *Amiotte Suchet and Probst* [1993b]). Slope values of the linear models are 0.095 for shield rocks, 1.586 for carbonate rocks, 0.222 for acid volcanic rocks, 0.479 for basalts, 0.152 for sands and sandstones (not represented in the figure) and 0.627 for shales (not represented in the figure).

Table 5. Global Budget of Atmospheric/Soil CO_2 Consumed by Weathering and Corresponding Alkalinity for Each Lithological Class[a]

	Sands and Sandstones	Shales	Carbonate Rocks	Shield Rocks	Acid Volcanic Rocks	Basalts	Total
Atmospheric/soil CO_2 consumed, F_T	1.10	8.57	8.63	1.50	0.21	1.49	21.49
Atmospheric/soil CO_2 consumed, F_S	30.92	250.84	478.26	40.36	67.31	215.04	159.46
River alkalinity (HCO_3^-), F_T	1.10	8.57	17.26	1.50	0.21	1.49	30.11
River alkalinity (HCO_3^-), F_S	30.92	250.84	956.53	40.36	67.31	215.04	223.48
Area, 10^6 km^2	35.42	34.16	18.03	37.13	3.05	6.94	134.74
Drainage intensity, $mm.yr^{-1}$	195.73	400.06	301.55	424.85	303.18	448.94	340.32
Percent of total CO_2 consumed worldwide	5.10	39.88	40.14	6.98	0.96	6.95	100.00
Percent of the world area	26.3	25.3	13.4	27.6	2.3	5.1	100.00

[a]Calculations include exoreic and endoreic area; F_T, total annual flux in 10^{12} moles yr^{-1}; FS, specific annual flux in 10^3 moles km^{-2} yr^{-1}.

carbonate minerals so that at the continental scale, this proportion is very difficult to estimate. On average, *Garrels and Mackenzie* [1971] estimated the proportion of carbonate minerals to be about 6%. Even so, the validation of GEM-CO2 on large river basins shows that calculated alkalinity fluxes are very close to observed fluxes [*Amiotte Suchet and Probst*, 1995; *Ludwig et al.*, 1998]. This is probably because the weathering CO_2 consumption rate of shales is intermediate between carbonates and shield rocks; consequently, the overestimations could compensate locally for the underestimations.

4.2. Global Budget of Atmospheric/Soil CO_2 Consumed by Different Rock Types

[24] Using GEM-CO2, a global budget of atmospheric/soil CO_2 consumption has been established for each rock type (Table 5). First, it can be observed that CO_2 consumption by carbonate rocks accounts for 40% of the worldwide atmospheric/soil CO_2 uptake and supplies 57% of the total alkalinity river input to the ocean, even if carbonates cover only 13% of the total continental area. Keeping in mind that the carbonate dissolution on the continent is balanced by the carbonate precipitation in the ocean, the carbonate weathering on land should have no effect on the CO_2 budget in the atmosphere.

[25] The remaining 60% of CO_2 uptake is attributed to silicate rock weathering which can also precipitate as carbonate in the ocean, but only pro parte according to the availability of calcium plus magnesium released by silicate weathering. Thus, it is important to distinguish among the silicates the contribution of the different rock types to the global atmospheric/soil CO_2 uptake. Shales (29% of the silicate rock outcrops) account for 40% of the total CO_2 consumed worldwide and almost 67% of the total CO_2 consumed by weathering of silicate rocks. Weathering of sands/sandstones or shield rocks, which are as abundant as shales, consumes a much lower proportion of atmospheric/soil CO_2 (about 5% and 7%, respectively), while weathering of basalts (only 5% of the continental area) represents almost 7% of the global weathering CO_2, and 12% of CO_2 consumed by silicate weathering only.

[26] A CO_2 and alkalinity transport budget by lithology can also be established for the 39 major world river basins (Table 6). The results show a wide variety of situations in which F_{CO2} and alkalinity fluxes reflect the drainage intensity and the lithological composition of the drainage basin as well.

[27] Figure 6 compares observed and calculated alkalinity (HCO_3^-) fluxes for most of the 39 selected basins. As already mentioned by *Ludwig et al.* [1998], this comparison gives best results for rivers in tropical wet climate, whereas for other rivers, GEM-CO2 underestimates alkalinity fluxes. This is especially surprising for temperate wet rivers because the empirical relationships of the model were based upon data of watersheds located in the temperate wet climate. This may be explained by the fact that, at the scale of large river basin, these watersheds represent more the headwater regions with a small residence time of the water. So, the model fits best in tropical wet climate where the very humid climate leads to a low residence time of the water in the basin. As the residence time of water becomes higher, the chemical concentration of water increases and fluxes are higher. *Ludwig et al.* [1998] have shown that, after correction using a climatic factor, fluxes were fitted well.

[28] Figure 4 allows us to analyze the relations between the lithology of the large river basins and their weathering CO_2 consumption rates. It appears that most of the drainage basins dominated by weathering resistant rocks (shield rocks, acid volcanic rocks, sands and sandstones outcrops >60%) exhibit the lowest weathering CO_2 fluxes (less than 50 10^3 moles km^{-2} yr^{-1}) and alkalinity river transports (less than 60 $\times$ 10^3 moles km^{-2} yr^{-1}). Concerning the other drainage basins, those dominated by carbonate rocks (easily weathered rock outcrop >20%) show generally higher weathering CO_2 uptake and alkalinity river fluxes (200 to 1150 $\times$ 10^3 moles km^{-2} $yr^{-1}$and 360 to 2292 $\times$ 10^3 moles km^{-2} yr^{-1}, respectively) than those dominated by intermediate rocks (basalts and shales outcrops > 50%; 50 to 200 $\times$ 10^3 moles km^{-2} yr^{-1} and 60 to 226 $\times$ 10^3 moles km^{-2} yr^{-1}, respectively). However, this trend is modulated by the influence of the runoff: For example, the Amazon and Orinoco river basins (basins number 1 and 27, respectively) show high weathering CO_2 fluxes whereas few carbonate rocks outcrop in their drainage basin. Inversely, the Tigris-Euphrate river (basin number 34), characterized by large carbonate rock outcrops, shows moderate weathering CO_2 fluxes because of its low runoff. The average CO_2 consumption by weathering in the 39 selected basins distributed by rock type shows the same pattern as that determined in Table 5 for the whole land areas, excepted for basalts, which contribute to only 3.6% of the CO_2 consumed by rock weathering in the selected basins compared to about 7% of the CO_2 consumed worldwide.

Table 6. Budget of Atmospheric/Soil CO_2 Consumed by Weathering of Main Rock Types for 39 Major River Basins of the World as Calculated by GEM-CO2

			CO_2 Consumed by Weathering of (Percent of Total Consumed)							Flux of Consumed CO_2, 10^3 moles km^{-2} yr^{-1}			Flux of Alkalinity,[a] 10^3 moles km^{-2} yr^{-1}	
	Basin No.	Area (10^6 km^2)	Sands and Sandstone	Shales	Carb. Rocks	Shield Rocks	Acid Volcanic Rocks	Basalts	All Silicate Rocks	Total River Basin	Silicate Rock	Carb. Rocks	Total Calculated (1)	Total Observed (2)
Amazon	1	5.83	4.0	76.1	14.4	4.8	0.6	0.0	85.6	509.49	435.96	73.53	583.03	462.0
Amour	2	1.87	4.3	59.3	0.0	23.7	0.0	12.7	100.0	54.85	54.85	0.00	54.85	124.0
Colorado	3	0.67	79.6	0.0	0.0	11.4	9.0	0.0	100.0	6.31	6.31	0.00	6.31	67.0
Columbia	4	0.62	0.4	52.8	0.0	16.8	14.1	15.9	100.0	119.88	119.88	0.00	119.88	374.0
Danube	5	0.74	1.8	38.5	56.9	2.8	0.0	0.0	43.1	136.44	58.82	77.62	214.05	
Don	6	0.39	0.0	81.2	18.8	0.0	0.0	0.0	81.2	55.88	45.39	10.50	66.38	
Fraser	7	0.24	0.0	89.3	0.0	7.6	3.1	0.0	100.0	187.16	187.16	0.00	187.16	390.0
Ganges-Brahmaputra	8	1.64	7.4	31.3	55.9	5.1	0.0	0.4	44.1	430.48	190.03	240.46	670.94	1116.0
Godavari	9	0.30	3.2	0.0	0.0	42.3	0.0	54.5	100.0	85.08	85.08	0.00	85.08	474.0
Huangho	10	0.79	8.2	1.5	65.2	25.1	0.0	0.0	34.8	14.60	5.08	9.52	24.13	235.0
Yenisei	11	2.44	2.2	16.1	44.4	6.5	0.0	30.9	55.6	136.27	75.80	60.47	196.74	279.0
Indigirka	12	0.34	23.6	76.4	0.0	0.0	0.0	0.0	100.0	58.55	58.55	0.00	58.55	
Indus	13	0.88	4.8	6.7	71.5	17.0	0.0	0.0	28.5	107.91	30.74	77.16	185.07	654.0
Irrawaddi	14	0.40	5.1	14.6	78.3	2.0	0.0	0.0	21.7	906.50	196.84	709.66	1616.16	
Kolyma	15	0.59	54.4	45.6	0.0	0.0	0.0	0.0	100.0	49.35	49.35	0.00	49.35	
Lena	16	2.32	6.1	31.8	42.3	14.1	0.0	5.7	57.7	61.26	35.35	25.91	87.17	237.0
Limpopo	17	0.31	8.2	0.0	50.4	19.5	0.0	21.9	49.6	25.96	12.87	13.09	39.05	37.0
Mackenzie	18	1.47	0.0	61.9	35.0	3.1	0.0	0.0	65.0	115.28	74.91	40.38	155.66	291.0
Magdalena	19	0.26	10.4	41.1	25.7	6.6	16.3	0.0	74.3	422.53	314.07	108.47	531.00	703.0
Mekong	20	0.82	1.9	36.6	50.4	3.7	1.3	6.1	49.6	476.77	236.59	240.18	716.94	526.0
Mississippi	21	3.13	4.7	38.9	54.9	1.4	0.2	0.0	45.1	128.71	58.06	70.64	199.35	309.0
Murray	22	1.11	2.8	71.1	0.0	11.6	7.3	7.3	100.0	12.03	12.03	0.00	12.03	
Niger	23	1.50	42.3	0.0	21.2	35.4	0.0	1.1	78.8	16.86	13.28	3.58	20.44	72.0
Nile	24	1.84	4.1	0.0	25.5	6.6	0.0	63.7	74.5	27.73	20.66	7.07	34.80	122.0
Ob	25	3.01	7.0	80.6	5.0	0.2	0.0	7.2	95.0	82.34	78.22	4.13	86.47	236.0
Orange	26	0.66	35.7	0.0	11.9	0.8	0.0	51.6	88.1	11.21	9.88	1.33	12.54	27.0
Orinoco	27	0.96	7.2	69.9	1.6	15.3	0.0	5.9	98.4	238.06	234.25	3.81	241.87	219.0
Parana	28	2.84	17.6	33.9	3.5	7.9	0.1	37.1	96.5	71.57	69.10	2.47	74.04	119.0
Sao Francisco	29	0.59	3.1	7.0	86.9	3.0	0.0	0.0	13.1	171.20	22.40	148.80	320.00	
Senegal	30	0.36	62.8	2.3	0.0	15.2	0.0	19.7	100.0	6.97	6.97	0.00	6.97	
Severnaia Dvina	31	0.30	2.7	70.8	26.5	0.0	0.0	0.0	73.5	218.21	160.30	57.90	276.11	798.0
Si Kiang	32	0.44	0.0	0.0	98.1	1.9	0.0	0.0	1.9	1156.77	21.52	1135.25	2292.02	1411.0
St. Lawrence	33	0.87	0.0	5.7	80.4	13.8	0.0	0.0	19.6	200.64	39.23	161.41	362.05	600.0
Tigris-Euphrates	34	0.93	2.7	16.2	72.5	0.2	7.9	0.5	27.5	131.28	36.04	95.23	226.51	
Yana	35	0.21	25.2	74.8	0.0	0.0	0.0	0.0	100.0	43.44	43.44	0.00	43.44	71.0
Yangtze-Kiang	36	1.74	2.1	5.6	89.0	3.3	0.0	0.0	11.0	463.05	50.86	412.18	875.23	921.0
Yukon	37	0.78	0.0	98.1	0.0	1.9	0.0	0.0	100.0	123.44	123.44	0.00	123.44	467.0
Zaire	38	3.60	35.4	0.0	51.3	11.9	0.0	1.4	48.7	93.68	45.60	48.08	141.76	82.3
Zambesi	39	1.31	13.9	0.0	73.8	9.7	0.0	2.7	26.2	34.52	9.06	25.46	59.98	29.0
39 selected basins		49.11	5.7	43.4	41.1	5.6	0.7	3.6	58.9	186.80	110.12	76.68	263.48	
Arctic Ocean		16.34	3.9	49.4	34.3	4.0	0.0	8.2	65.7	99.56	65.38	34.19	133.75	
North Atlantic		26.33	4.3	50.1	32.7	8.5	0.7	3.7	67.3	227.14	152.84	74.30	301.44	
South Atlantic		17.08	20.8	17.0	31.0	16.2	1.1	13.9	69.0	89.92	62.04	27.88	117.80	
Pacific Ocean		20.07	2.7	43.4	38.0	5.5	1.2	9.2	62.0	334.57	207.36	127.21	461.78	
Indian Ocean		16.14	6.3	19.4	62.2	5.2	0.9	6.0	37.8	213.52	80.61	132.91	346.43	
Mediterranean		6.56	1.6	33.2	59.3	1.7	0.5	3.6	40.7	150.00	61.12	88.88	238.88	
Below 60° south		1.73	0.5	33.4	0.0	21.2	15.0	29.9	100.0	74.02	74.02	0.00	74.02	

[a](1) calculated by GEM-CO2, this study, (2) taken from a compilation of literature data by *Ludwig et al.* [1998].

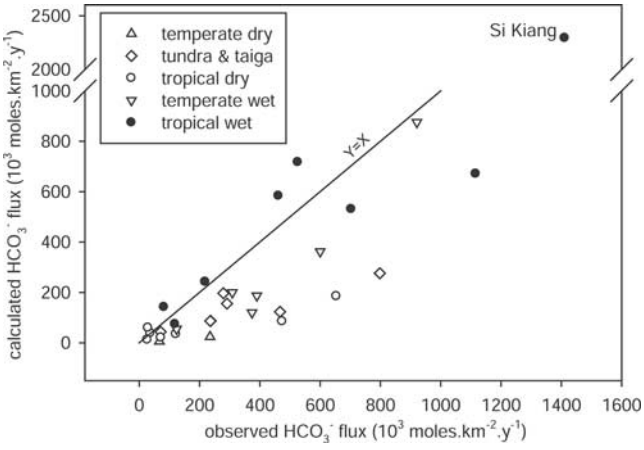

Figure 6. Comparison of the observed HCO_3^- fluxes with the fluxes calculated with GEM-CO2 (see data in Table 6).

[29] For the ocean basins (Table 6), the distribution is much more homogeneous: About two thirds of the weathering CO_2 fluxes and half of the river alkalinity input originate from silicate rocks for the Arctic, North and South Atlantic and Pacific Oceans, whereas, for the Mediterranean Sea and the Indian Ocean, the contribution of silicate rock weathering represents only about 40% and 25%, respectively, for the overall CO_2 flux and alkalinity river input.

[30] If we look at the latitudinal distributions of weathering CO_2 consumption by the different rock types (Figure 7), it appears clear that weathering of shales represents a major sink for atmospheric/soil CO_2 ($0.4-1.8 \times 10^{12}$ moles yr^{-1} per 5° latitude) in the Northern Hemisphere between 35° and 70° and in the Southern Hemisphere between 5° and 40°, even if the shales outcrop are less abundant than the shield ones. Concerning the other rock type, the latitudinal weathering CO_2 fluxes follow more or less the outcrop areas, except for sands and sandstones between 25°S and 15°N and between 35°N and 55°N, for carbonate rocks between 15°S and 10°N and for acid volcanic rocks between 0° and 10°N and between 30°S and 45°S. Most of these exceptions can be attributed to high or low drainage intensities at the corresponding latitudes.

5. Conclusion

[31] A compilation of lithological, soil and geological maps available for regional and continental areas allowed us in this study to construct for the first time a world lithological map with a grid resolution of $1° \times 1°$. The basis data of this lithological map are now available on a website (http://www.obs-mip.fr/omp/umr5563/4equ/hg/IGCP459/litho.html) and can be used for future studies on global biogeochemical cycles, particularly for chemical weathering and fluvial transports of dissolved elements into the oceans. This work gives, for the first time on a global scale, access to the spatial distribution of the main rock types with regard to their chemical weathering rate: plutonic and metamorphic rocks (shield rocks), acid volcanic rocks, basalts, sands and sandstones, shales and carbonates. Unfortunately, evaporitic rocks could not be taken into account because their outcropping areas are always very limited.

[32] The worldwide outcrops of each rock type that could be calculated from these data are comparable to previous estimates [*Blatt and Jones*, 1975; *Meybeck*, 1987]: Two thirds of the continental rocks are sedimentary rocks (sands and sandstones, shales and carbonates), of which carbonates represent only 20%, and one third are crystalline rocks (intrusive igneous and metamorphic, acid volcanic and basalts). Basalts represent only 15% of the total crystalline rocks area. A careful analysis of the spatial distribution of each rock type shows that shield rocks and sands/sandstones are equally distributed over the latitudes, contrary to the other rocks. Indeed, carbonates are more abundant in the Northern Hemisphere between 20°N and 40°N and between 70°N and 90°N, shales are more abundant between 30°N and 70°N and between 0° and 40°S, half of the acid volcanic rocks outcrops between 20°N and 50°N, and 70% of basalt areas stretch out between 0° and 30°N and between 50°N and 70°N and between 20°S and 30°S, corresponding to large areas of basaltic traps. If we look at the spatial distribution by continents, there also appear to be some discrepancies: Most of the sands and sandstones are located in Africa and in Asia covering pro parte endoreic areas. Shales are poorly represented in Africa, carbonates are quite sparse in Australia and South America, basalts are poorly represented in Europe and in North America, and finally, acid volcanic rocks are highly represented in North and South America and in Australia. Looking at the different ocean drainage basins, the distribution appears to be more homogeneous, except for volcanic rocks. Thus, the rivers flowing into the Pacific Ocean and below 60°S are draining land areas where acid volcanic rocks are more abundant, and the Indian Ocean drainage basin is enriched in basalts.

[33] An average lithological composition could be also calculated for 39 large river basins showing that the total land area drained by these rivers is representative of the world distribution. Nevertheless the abundance of each rock type is greatly variable from one drainage basin to another. Consequently, some river basins (carbonate outcrop abundance greater than 20%) appear to be very sensitive to the chemical weathering and present high weathering CO_2 consumption rates while some others (outcrop abundance of shields, sands and sandstones greater than 60%, with less than 20% of carbonates) appear to be very resistant to chemical alteration and present low CO_2 consumption rates. Drainage basins where the outcrop abundance of shales and basalts represent more than 40% and carbonates less than 20% are intermediate between the previous two groups.

[34] As we have already shown in previous works [*Amiotte Suchet and Probst*, 1993a, 1993b, 1995], the flux of CO_2 consumed by rock weathering is greatly variable according to the rock types: Shield rocks present the lowest values, and the CO_2 flux consumed by sands/sandstones, acid volcanic rocks, basalts, shales and carbonates are respectively 1.5, 2.3, 5.0, 6.6 and 16.7 times greater than the CO_2 flux consumed by shield rocks. Consequently, the relative outcrop abundance of the different rock types as well as their spatial distribution in relation to the latitudinal

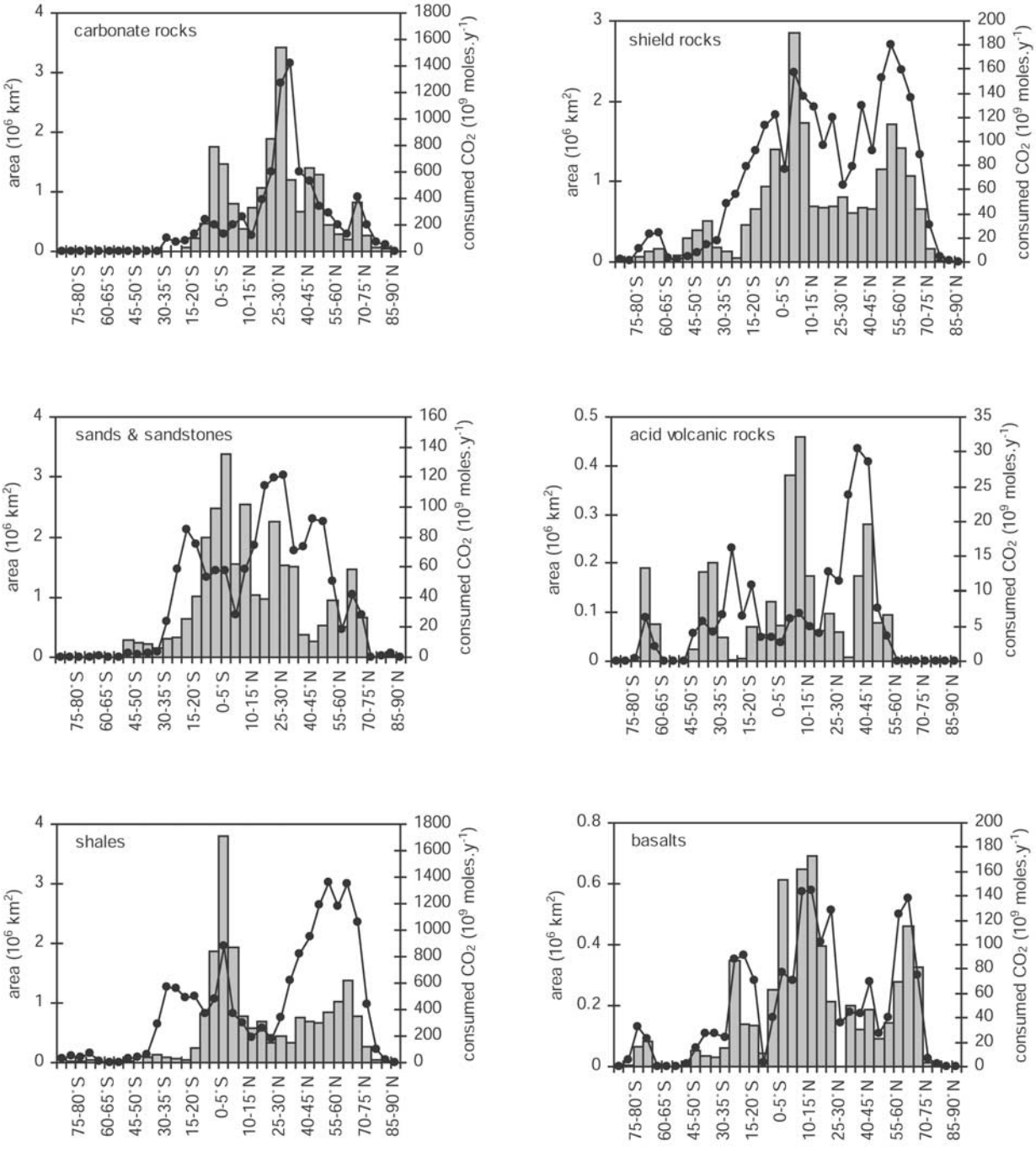

Figure 7. Latitudinal distribution of the weathering CO_2 consumption by rock type. The curve represents the outcrop areas.

and altitudinal variations of the main hydroclimatic factors (precipitation, runoff and temperature) have a great influence on the global CO_2 consumed by rock weathering and on the riverine transports of dissolved elements into the oceans. Coupling the GEM-CO_2 modeling [*Amiotte Suchet and Probst*, 1995] with the spatial distribution of the different rock types, it was possible in this study to estimate for each large river basin and for the global scale, the CO_2 uptake by each rock type. The dissolution of carbonates and the chemical alteration of shales consume both 80% (40% each) of the total CO_2 uptake by continental weathering, even if their respective outcrop area represent only 13% and 25% of the total land area. On the contrary, sands, sandstones and shield rocks consume a total of only 12% (5%

and 7%, respectively) of the total CO_2 uptake while their outcrop areas occupy 54% of the continents (26% and 28%, respectively). Finally, the contribution of volcanic rock (acid and basalts) weathering to the total CO_2 flux (8%) is proportional to their outcrop abundance (7%). Nevertheless, the chemical alteration of basalts which cover only 5% of the total land areas represents 7% of the total CO_2 uptake.

[35] Consequently, by combining large areas of shales (even if they may contain a small amount of carbonate mineral) or basalts with high temperature and high runoff intensity must lead to high weathering CO_2 consumption, which could play a significant role in the CO_2 content in the atmosphere and consequently in the global climate on Earth, as recently shown by *Dessert et al.* [2001] for the Deccan Traps 65.5 Myr ago. In the same way, during glacial periods, huge ice sheets and large areas of emerging continental shelves must change the proportion and the spatial distribution of the main lithologies and consequently could have a great influence on the weathering CO_2 flux and on the riverine transports of dissolved elements, as proposed by *Gibbs and Kump* [1994] and *Ludwig et al.* [1998] for the Last Glacial Maximum (18,000 years BP).

[36] **Acknowledgments.** This work was funded by the Environment and Climate Program of the European Community (ESCOBA-Biosphere contract ENV-CT95-0111). This paper is a contribution to the working group "Weathering as a Carbon Sink" of the "INQUA Commission on Carbon" and to IGCP Projects 404 ("Terrestrial Carbon in the Past 125 ka") and 459 ("Carbon Cycle and Hydrology in the Paleo-Terrestrial Environments").

References

Amiotte Suchet, P., and J. L. Probst, Flux de CO_2 atmosphérique consommé par altération chimique continentale: Influence de la nature de la roche, *C. R. Acad. Sci., Ser. II*, *317*, 615–622, 1993a.

Amiotte Suchet, P., and J. L. Probst, Modelling of atmospheric CO_2 consumption by chemical weathering of rocks: Application to the Garonne, Congo and Amazon basins, *Chem. Geol.*, *107*, 205–210, 1993b.

Amiotte Suchet, P., and J. L. Probst, A global model for present day atmospheric/soil CO_2 consumption by chemical erosion of continental rocks (GEM-CO_2), *Tellus, Ser. B*, *47*, 273–280, 1995.

Aumont, O., J. C. Orr, P. Monfray, W. Ludwig, P. Amiotte Suchet, and J. L. Probst, Riverine-driven interhemispheric transport of carbon, *Global Biogeochem. Cycles*, *15*, 393–405, 2001.

Berner, R. A., A. C. Lasaga, and R. M. Garrels, The carbonate-silicate geochemical cycle and its effect on atmospheric carbon dioxide over the past 100 millions years, *Am. J. Sci.*, *283*, 641–683, 1983.

Blatt, H., and R. L. Jones, Proportions of exposed igneous, metamorphic and sedimentary rocks, *Geol. Soc. Am. Bull.*, *86*, 1085–1088, 1975.

Bluth, G. J. S., and R. L. Kump, Phanerozoic paleogeology, *Am. J. Sci.*, *291*, 281–308, 1991.

Choubert, G., and A. Faure-Mauret, Atlas géologique du monde, map, 32 sheets, Comm. de la Carte Géol. du Monde, Bur. de Cartogr. Géol. Int., U. N. Educ. Sci. and Cult. Org., Paris, 1981.

Clarke, F., The data of geochemistry, *U.S. Geol. Surv. Bull.*, *770*, 841, 1924.

Dessert, C., B. Dupré, L. M. François, J. Schott, J. Gaillardet, G. Chakrapani, and S. Bajpai, Erosion of Deccan Traps determined by river geochemistry: Impact on the global climate and the $^{87}Sr/^{86}Sr$ ratio of seawater, *Earth Planet. Sci. Lett.*, *188*, 459–474, 2001.

Food and Agriculture Organization—U.N. Educational, Scientific, and Cultural Organization (FAO-UNESCO), *Soil Map of the World*, 10 vols., U. N. Educ. Sci. and Cult. Org., Paris, 1981.

Gaillardet, J., B. Dupré, P. Louvat, and C. J. Allègre, Global silicate weathering and CO_2 consumption rates deduced from the chemistry of the large rivers, *Chem. Geol.*, *159*, 3–30, 1999.

Garrels, R. M., and F. T. Mackenzie, *Evolution of Sedimentary Rocks*, 397 pp., W. W. Norton, New York, 1971.

Gibbs, M. T., and L. R. Kump, Global chemical erosion during the last glacial maximum and the present: Sensitivity to changes in lithology and hydrology, *Paleoceanography*, *9*, 529–543, 1994.

Khain, V. E., A. B. Ronov, and A. N. Balukhovskiy, Cretaceous lithologic associations of the world (Engl. transl.), *Int. Geol. Rev.*, *18*, 1269–1295, 1975.

Korzoun, V. I., A. A. Sokolov, M. I. Budyko, G. P. Voskresensky, A. A. Kalinin, E. S. Konoplyantsev, E. S. Korotkevich, and M. I. Lvovich, *Atlas of World Water Balance*, U. N. Educ. Sci. and Cult. Org., Paris, 1977.

Ludwig, W., J. L. Probst, and S. Kempe, Predicting the oceanic input of organic carbon by continental erosion, *Global Biogeochem. Cycles*, *10*, 23–41, 1996.

Ludwig, W., P. Amiotte Suchet, G. Munhoven, and J. L. Probst, Atmospheric CO_2 consumption by continental erosion: Present-day control and implications for the Last Glacial Maximum, *Global Planet. Change*, *16–17*, 107–120, 1998.

Ludwig, W., P. Amiotte Suchet, and J. L. Probst, Enhanced chemical weathering of rocks during the Last Glacial Maximum: A sink of atmospheric CO_2?, *Chem. Geol.*, *159*, 147–151, 1999.

Meybeck, M., Global chemical weathering of surficial rocks estimated from river dissolved loads, *Am. J. Sci.*, *287*, 401–428, 1987.

Peters, N. E., Evaluation of environmental factors affecting yields of major dissolved ions of streams in the United States, *U.S. Geol. Surv. Water Supply Pap.*, *2228*, 39 pp., 1984.

Pinet, P., and M. Souriau, Continental erosion and large scale relief, *Tectonics*, *7*, 563–582, 1988.

Ronov, A. B., and V. E. Khain, Triassic lithologic association of the World (in Russian), *Sov. Geol.*, *1*, 32–46, 1961.

Ronov, A. B., and A. A. Yaroshevskyi, Earth crust geochemistry, in *Encyclopedia of Geochemistry and Environmental Sciences*, edited by R. Fairbridge, pp. 243–254, Van Nostrand Reinhold, New York, 1972.

Ronov, A. B., and A. A. Yaroshevskyi, A new model for the chemical structure of the Earth crust, *Geochem. Int.*, *13*, 1761–1795, 1976.

Ronov, A. B., V. E. Khain, and A. N. Balukhovskiy, Palegene lithologic associations of the continents (Engl. transl.), *Int. Geol. Rev.*, *21*, 415–446, 1979.

P. Amiotte Suchet, Microbiologie et Géochimie des Sols, UMR INRA, Université de Bourgogne, Centre des Sciences de la Terre, 6 bd Gabriel, F-21000 Dijon, France. (philippe.amiotte-suchet@u-bourgogne.fr)

W. Ludwig, Centre de Formation et de Recherche sur l'Environnement Marin, UMR 5110, Université de Perpignan, 52, avenue de Villeneuve, F-66860 Perpignan Cedex, France. (ludwig@univ-perp.fr)

J.-L. Probst, Laboratoire des Mécanismes de Tranfert en Géologie, UMR CNRS/Université Paul Sabatier 5563, 38 rue des 36 Ponts, F-31400 Toulouse, France. (jlprobst@cict.fr)

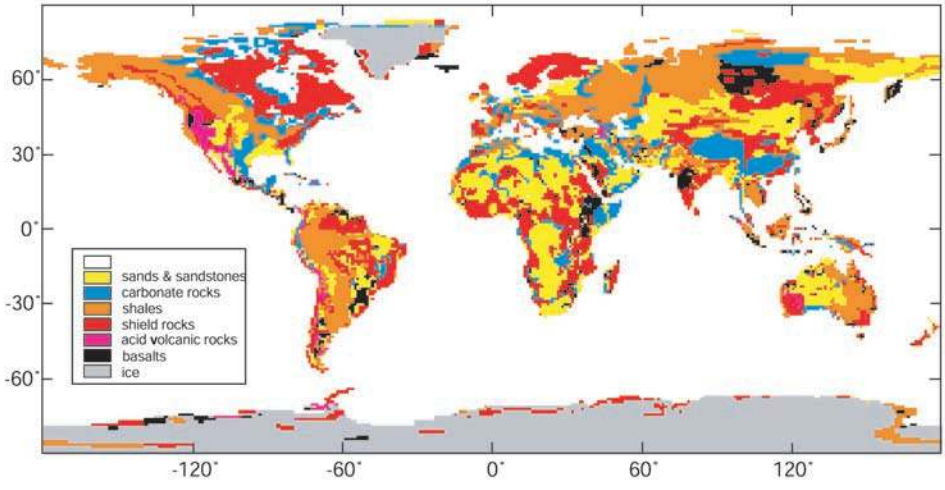

Figure 1. Present-day exposures of the six major rock types on land area ($1^\circ \times 1^\circ$ resolution).